and placed in mesocosms. On termination of the experiment these macrofauna were retrieved and enumerated. We analysed the data by ANCOVA. The contribution of each species to variation in NH_4-N production as biomass increased was assessed by multiple regression. This allows for the identification of species that might be regarded as causing a sampling effect, but does not allow for the determination of a diversity effect such as over yielding.

Null model

We used observations derived from single-species regression slopes to generate an additive null mixture regression slope against which to compare observed responses from multi species mixtures. The null model was of the form $E(j) = (\Sigma_{i=1}^{n}(\alpha_i p_i j + b_i) - M_{iZERO}) + M_{ZERO}$ where $E(j)$ is the expected multispecies response at biomass j; p_i is the proportion of species i represented in mixture by biomass; α_i is the slope of the regression line defining the relationship between biomass and ecosystem response for species i; and b_i is the intercept of the regression line defining the relationship between biomass and ecosystem response for species i. M_{ZERO} is the mean, observed ecosystem response at zero biomass. It is important to distinguish between additive and substitutive experimental designs[25]; the null model approach detailed here is of an additive statistical design, whereas calculation of metrics such as D_{Max} (over yielding) requires a substitutive experimental design. The experimental approach we have developed here allows for exploration of both approaches.

Received 24 November 2000; accepted 29 January 2001.

1. Naeem, S. & Li, S. Biodiversity enhances ecosystem reliability. *Nature* **390,** 507–509 (1997).
2. Tilman, D., Lehman, C. L. & Thompson, K. T. Plant diversity and ecosystem productivity: theoretical considerations. *Proc. Natl Acad. Sci. USA* **94,** 1857–1861 (1997).
3. Hooper, D. U. The role of complementarity and competition in ecosystem responses to variation in plant diversity. *Ecology* **79,** 704–719 (1998).
4. Hector, A. *et al.* Plant diversity and productivity experiments in European grasslands. *Science* **286,** 1123–1127 (1999).
5. Wardle, D. A., Bonner, K. I. & Barker, G. M. Stability of ecosystem properties in response to above-ground functional group richness and composition. *Oikos* **89,** 11–23 (2000).
6. McGrady-Steed, J., Harris, P. M. & Morrin, P. J. Biodiversity regulates ecosytem predictability. *Nature* **390,** 162–165 (1997).
7. McGrady-Steed, J. & Morin, P. J. Biodiversity, density compensation and the dynamics of populations and functional groups. *Ecology* **81,** 361–373 (2000).
8. Huston, M. *et al.* No consistent effect of plant diversity on productivity. *Science* **289,** 1255–1257 (2000).
9. Hector, A. *et al.* No consistent effect of plant diversity on productivity–response. *Science* **289,** 1257–1259 (2000).
10. Wardle, D. *et al.* Biodiversity and ecosystem function: an issue in ecology. *Bull. Ecol. Soc. Am.* **81,** 235–239 (2000).
11. Naeem, S. Reply to Wardle et al. *Bull. Ecol. Soc. Am.* **81,** 241–246 (2000).
12. Wardle, D. A., Bonner, K. I. & Nicholson, K. S. Biodiversity and plant litter: experimental evidence which does not support the view that enhanced species richness improves ecosystem function. *Oikos* **80,** 470–480 (1997).
13. Nixon, S. W. in *Estuaries and nutrients* (eds Neilson, B. J. & Cronin, L. E.) 111–138 (Humana, Cliftown, 1981).
14. Nedwell, D. B., Jickells, T. D., Trimmer, M. & Sanders, R. Nutrients in estuaries. *Adv. Ecol. Res.* **29,** 43–92 (1999).
15. Yachi, S. & Loreau, M. Biodiversity and ecosystem productivity in a fluctuating environment: The insurance hypothesis. *Proc. Natl Acad. Sci. USA* **96,** 1463–1468 (1999).
16. Ives, A. R., Gross, K. & Klug, J. L. Stability and variability in competitive communities. *Science* **286,** 542–544 (1999).
17. Hughes, J. B. & Roughgarden, J. Species diversity and biomass stability. *Am. Nat.* **155,** 618–627 (2000).
18. Loreau, M. Separating sampling and other effects in biodiversity experiments. *Oikos* **82,** 600–602 (1998).
19. Hector, A. The effect of diversity on productivity: detecting the role of species complementarity. *Oikos* **82,** 597–599 (1998).
20. Emmerson, M. C. & Raffaelli, D. G. Detecting the effects of diversity on measures of ecosystem function: experimental design, null models and empirical observations. *Oikos* **91,** 195–203 (2000).
21. Tilman, D. Causes, consequences and ethics of biodiversity. *Nature* **405,** 208–211 (2000).
22. Lawton, J. H., Naeem, S., Thompson, L. J., Hector, A. & Crawley, M. J. Biodiversity and ecosystem function: getting the Ecotron experiment in its correct context. *J. Func. Ecol.* **12,** 848–852 (1998).
23. Wardle, D. A. Is "sampling effect" a problem for experiments investigating biodiversity-ecosystem function relationships? *Oikos* **87,** 403–407 (1999).
24. Stachowicz, J. J., Whitlach, R. B. & Osman, R. W. Species diversity and invasion resistance in a marine ecosystem. *Science* **286,** 1577–1579 (1999).
25. Jolliffe, P. A. The replacement series. *J. Ecol.* **88,** 371–385 (2000).

Supplementary information is available on *Nature*'s World-Wide Web site (http://www.nature.com) or as paper copy from the London editorial office of *Nature*.

Acknowledgements

We thank L. Pihl and associated research staff at KMRS, Sweden and S. Hall and Flinders University for support in Australia. We also thank C. Biles and S. Way for help with fieldwork. Our work was supported by NERC and ESF grants to D.R. and D.P., and Carnegie trust to M.E.

Correspondence and requests for materials should be addressed to M.C.E. (e-mail: m.emmerson@abdn.ac.uk).

Larval dispersal potential of the tubeworm *Riftia pachyptila* at deep-sea hydrothermal vents

Adam G. Marsh*†, Lauren S. Mullineaux‡, Craig M. Young§ & Donal T. Manahan*

* *Department of Biological Sciences, University of Southern California, Los Angeles, California 90089, USA*
‡ *Biology Department, Woods Hole Oceanographic Institution, Woods Hole, Massachusetts 02543, USA*
§ *Division of Marine Science, Harbor Branch Oceanographic Institution, Fort Pierce, Florida 34946, USA*

Hydrothermal vents are ephemeral because of frequent volcanic and tectonic activities associated with crust formation[1–3]. Although the larvae of hydrothermal vent fauna can rapidly colonize new vent sites separated by tens to hundreds of kilometres[4,5], the mechanisms by which these larvae disperse and recruit are not understood. Here we integrate physiological, developmental and hydrodynamic data to estimate the dispersal potential of larvae of the giant tubeworm *Riftia pachyptila*. At *in situ* temperatures and pressures (2 °C and 250 atm), we estimate that the metabolic lifespan for a larva of *R. pachyptila* averages 38 days. In the measured flow regime at a fast-spreading ridge axis (9° 50′ N; East Pacific Rise), this lifespan results in potential along-ridge dispersal distances that rarely exceed 100 km. This limited dispersal results not from the physiological performance of the embryos and larvae, but instead from transport limitations imposed by periodic reversals in along-ridge flows and sustained episodes of across-ridge flow. The lifespan presented for these larvae can now be used to predict dispersal under current regimes at other hydrothermal vent sites.

Larval dispersal remains one of the most perplexing problems for understanding how hydrothermal vent organisms colonize vent sites[4,6]. We have surmounted a significant challenge to addressing this problem by successfully rearing embryos of *Riftia pachyptila* (Polychaeta: Siboglinidae) to the larval stage under deep-ocean temperatures and pressures. Using custom designed culture systems (Teflon-coated, stainless steel chambers with a continuous flow of seawater at 2 °C and 250 atm) we have followed the early development of *R. pachyptila* embryos and larvae.

Early cleavage (Fig. 1a–d) was similar to that of bathyal (600 m) siboglinids[7], except that embryos of *R. pachyptila* require higher pressure. After 34 d of development, we observed a swimming trochophore larval stage with two equatorial bands of simple cilia (Fig. 1e). As in the non-feeding larvae of another vestimentiferan worm, *Lamellibranchia* sp.[7], larvae of *R. pachyptila* did not develop a mouth through the first 34 d of development. Once cleavage was initiated (after the exclusion of two polar bodies), cells divided at an average rate of 1.8 d per division (Fig. 2a). Some fertilized eggs were returned to the vent site at 2,500 m in mesh-covered 50-ml culture tubes to develop *in situ* on the sea floor (2 °C). Rates of early development *in situ* were equivalent to those observed in pressure chambers (Fig. 2a).

Larvae of Antarctic echinoderms show a remarkable metabolic efficiency with larval lifespans potentially exceeding 1 yr at low temperatures (−1.5 °C)[8,9]. Larvae of hydrothermal vent organisms dispersing between vents at 2 °C might also have long metabolic lifespans. Larval lifespan is determined in part by the rate of energy use during development and the initial amount of energy available

† Present address: College of Marine Studies, University of Delaware, Lewes, Delaware 19958, USA.

in the egg. We measured metabolic rates at 2 °C and 250 atm in early embryos of *R. pachyptila* by end-point respirometry[10]. Developmental stages of *R. pachyptila* respired 5.1 ± 0.3 (mean ± s.e.) pmol O_2 per h per embryo and later stages (32–64 cells) averaged 17.8 ± 1.4 pmol O_2 per h per embryo (Fig. 2b). Biochemical analyses of the protein and lipid-class composition of eggs of *R. pachyptila* were conducted on samples from several females collected at different times of the year (Fig. 3a). To estimate a metabolic lifespan for developmental stages, we assumed that 50% of an egg's protein mass (34.5 ± 7.8 ng; mean ± s.d.) and 90% of its wax-ester lipid mass (144.4 ± 19.1 ng) could be metabolized (wax esters are used exclusively for energy storage in cold-water invertebrates)[11–13]. The average metabolic energy available for development was calculated to be 5.5 ± 0.8 μJ per egg (mean ± s.d., range 4.7–7.1 μJ). Balancing the cumulative rate of energy use during early development (Fig. 2b) with available energy, a typical larva of *R. pachyptila* could potentially survive for 38 d (range 34–44 d).

Knowing the potential metabolic lifespan of a larva of *R. pachyptila* solves only part of the dispersal distance puzzle. The solution also depends on the vertical and horizontal directions and distances larvae travel. Passive vertical movement of the eggs and early embryos of *R. pachyptila* has been suggested to be high (28 m d^{-1}, measured at 102 atm)[14]. However, our direct measurements of buoyancy in isolated pressure vessels with Plexiglass viewports revealed that eggs are near-neutrally buoyant at 250 atm (and 2 °C), with an average vertical velocity of only 2 m d^{-1} (Fig. 3b). At active hydrothermal venting sites, hot effluents mix with seawater to form buoyant plumes that rise until they cool to neutral buoyancy at a distance of 175–200 m above the bottom (in less than a day)[15,16]. Many early life stages of hydrothermal vent animals have been found entrained in this neutrally buoyant plume[17,18], and it is likely that eggs of *R. pachyptila* become entrained in this water mass as well.

At the height of the buoyant plume, the flow regime at our site (9° 50′ N, East Pacific Rise; EPR) was assessed over a period of one year with two long-term current records (April to December 1999 and December 1999 to April 2000) from an Aanderaa current meter positioned 175 m above bottom on the ridge axis near the 'Biovent' site (9° 50.9′ N, 104° 17.6′ W). The current velocities were variable, with periodicities at semi-diurnal, diurnal and fortnightly timescales. Residual flows tended to be oriented roughly along the

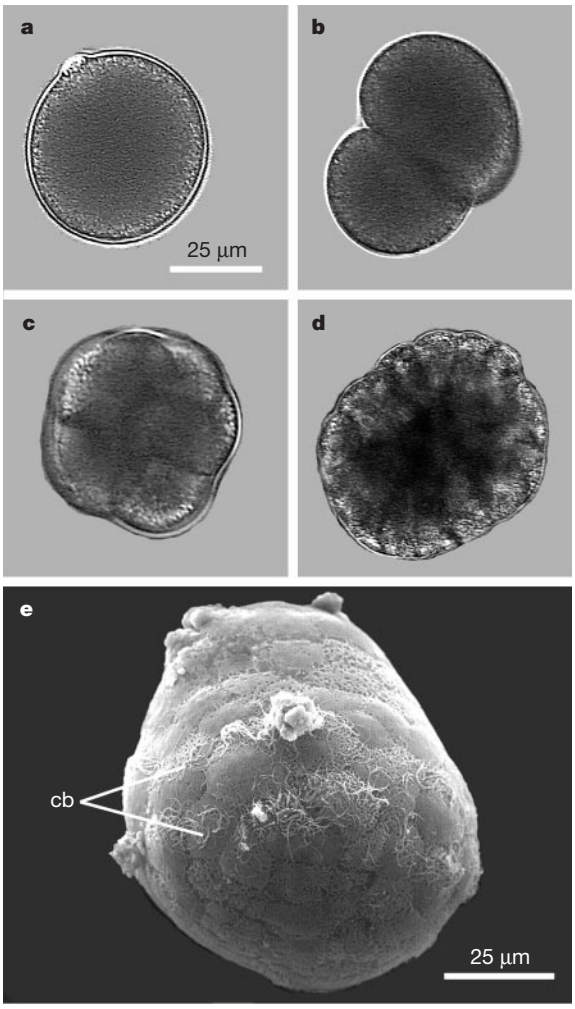

Figure 1 Early development to a larval stage in *Riftia pachyptila* cultured in pressure vessels at 2 °C and 250 atm. **a**–**d**, Light micrographs of first polar body extrusion (1 day; **a**), unequal blastomeres at the two-cell stage after polar lobe formation and first cleavage (3 days; **b**), the eight-cell stage (7 days; **c**), and a 128+ cell embryo (14 days; **d**). **e**, A scanning electron micrograph of a 34-day larva reveals two equatorial ciliary bands (cb) but no evidence of a mouth, apical tuft or other distinct morphological features.

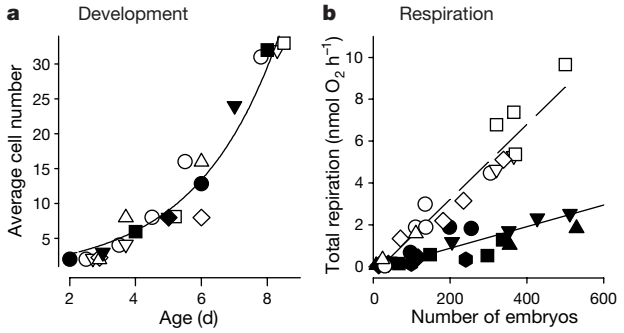

Figure 2 The developmental and respiration rates of *Riftia pachyptila* embryos. Symbols represent different cultures (different females, different cruises). **a**, For development, no difference was evident in cell division rates between cultures in pressure vessels (open symbols) or the *in situ* culture tubes (filled symbols). The combined regression of cell number against time ($y = 1.0283e^{(0.4299x)}$; $r^2 = 0.9623$) reveals a cleavage rate of 1.8 d per division. **b**, Embryo respiration measurements are divided into early (4–16 cells, filled symbols) and late (32–64 cells, open symbols) stages. Respiration rates of an individual embryo are determined as the slope from the linear regression equations: early $R = -0.147 + 0.00514x$, $r^2 = 0.9580$, $n = 19$; late $R = -0.354 + 0.0179x$, $r^2 = 0.9138$, $n = 18$. For later stages (> 20 d) a maximum metabolic rate of 21 pmol O_2 per h per individual was estimated from the rate of change in respiration during earlier development.

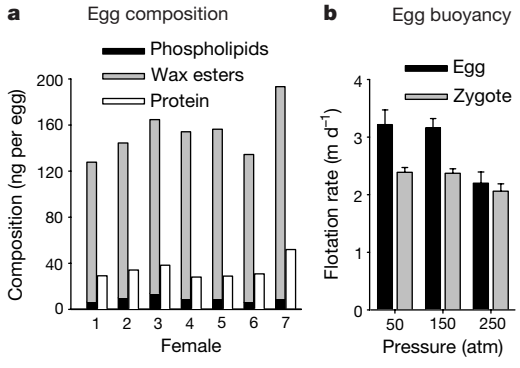

Figure 3 Biochemical composition and buoyancy of the eggs of *Riftia pachyptila*. **a**, Egg composition was assessed in different females, one from a cruise in May 1998, four from November 1998, and two from December 1999. Standard errors were less than 6% for the lipid assays and less than 2% for the protein assays, but are not plotted on the stacked histograms. **b**, Buoyancy was measured as flotation rates in pressurized vessels equipped with view ports for monitoring the vertical position of the eggs and zygotes (mean ± s.e.; sample sizes ranged from 62 to 223 observations per treatment).

NNW/SSE trending axis. The four-month current record from December 1999 to April 2000 gave evidence of a longer potential dispersal distance for larvae of *R. pachyptila*, which we have selected to present in detail.

To estimate dispersal potential of *R. pachyptila*, we modelled the movement of neutrally buoyant particles ('larvae') released at hourly intervals into the observed current regime. We followed each larval trajectory (Fig. 4b) for either a specified lifespan or until a larva had moved more than 25 km off axis (at which point it was considered 'lost' from the ridge system). During the four-month interval from December 1999 to April 2000 (Fig. 4a, b), larvae released at most time points experienced substantial cross-axis transport, with the exception of those released between 16 and 42 d after the current meter was used, when flow was consistently aligned SSW, roughly along the axis (Fig. 4b). Only a few combinations of release time and lifespan resulted in net dispersal distances greater than 100 km (only 0.9% of the releases); these occurred for larvae released on or shortly after day 16 with lifespans of 20–34 d (Fig. 4d). The maximum along-axis dispersal distance for any individual was 103.4 km SSE, and the furthest NNW any individual travelled was 47.3 km. In the eight-month current profile from April 1999 to December 1999, the longest dispersal distance SSE along-axis was only 54 km. Notably, the along-ridge flow reversals at our 9° N site result in a much higher probability that larvae will be retained within a few tens of kilometres of their source population, which might provide a mechanism of larval retention and rapid population growth at this site[5].

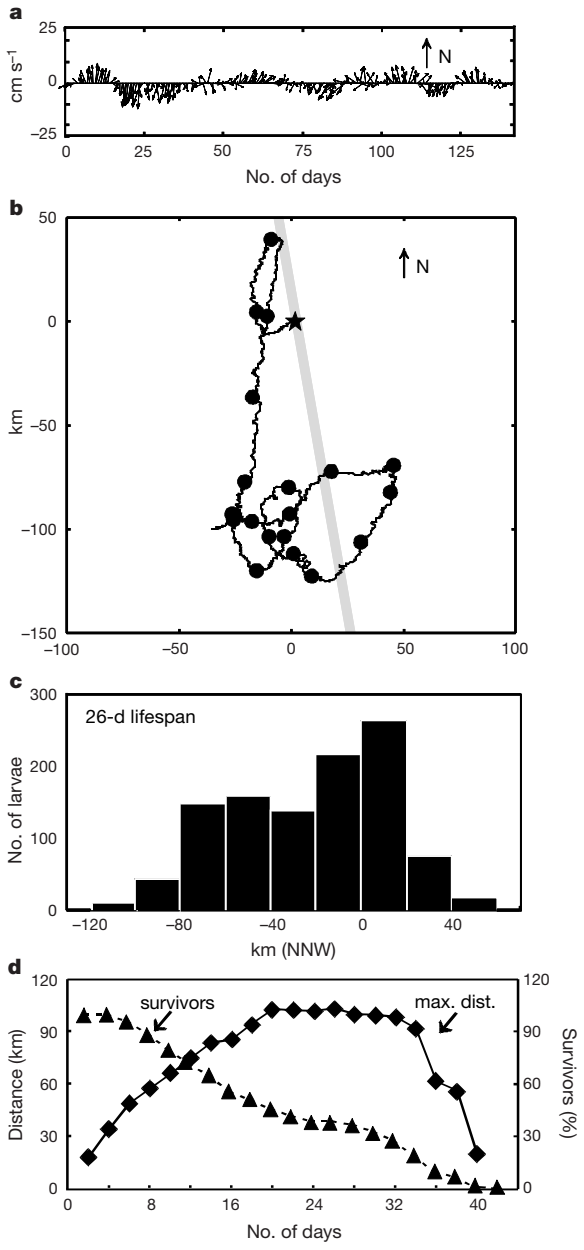

Figure 4 Dispersal potential of larvae of *Riftia pachyptila* modelled from current regimes at 9° N East Pacific Rise. **a**, Current velocities represented by arrows showing compass heading and velocity. **b**, Plan view of the trajectory of a water parcel, with its origin (star) at the location of the current meter and its path calculated from hourly-averaged velocities (filled circles denote positions at weekly intervals; grey line denotes the ridge axis). **c**, Along-axis distances (NNW is positive) travelled by larvae with a selected (26-d) lifespan released at hourly intervals in the 9° N current regime. Out of the 3,388 larval releases modelled, only 39% remained within 25 km of the ridge axis (these were termed 'survivors'). The maximum dispersal distance for a survivor with this 26-d lifespan was 103 km SSE. **d**, Maximum distance dispersed and percentage of survivors for larvae of each specified lifespan released in the dispersal model as described in **c**. For a lifespan greater than 42 d, no larval releases remained within 25 km of the ridge crest.

Contrary to expectations, a longer metabolic lifespan at 9° N EPR did not necessarily translate into a longer along-ridge dispersal distance. The more time a larva spent in the currents, the more likely it was to be swept off axis (Fig. 4d, 'survivors' curve). Sustained intervals of off-axis flow are characteristic of other sites on Eastern Pacific ridges[19,20], indicating that long-lived larvae probably have similar fates at these sites. Furthermore, mean along-axis velocities for extended ($\geq$ 40 d) intervals are typically less than 3 cm s^{-1} on Eastern Pacific ridges because of reversals in current direction[19–22]. These velocities would result in dispersal distances of less than 100 km for any larvae of *R. pachyptila* that remained near the ridge. An exception to this hydrodynamic limitation of dispersal occurs at 13° N EPR where periods of unidirectional, along-axis flow with mean velocity of 4.5 cm s^{-1} can last as long as 60 d (ref. 22). In this region, a longer lifespan of *R. pachyptila* larvae would result in substantially increased (up to 245 km) dispersal distances. It is also important to note that while off-axis flows impede dispersal along a ridge, they may be responsible for rare but important dispersal events to isolated vents (for example, on seamounts) or between ridges. In these cases, larval lifespan would limit the range and influence the frequency of successful colonization. Our data show the overriding importance of current flow in determining dispersal potential and suggest that populations at different vent sites may have different dispersal limits depending on local current conditions.

We have integrated physiological, developmental and hydrodynamic data into a specific dispersal estimate for larvae of *R. pachyptila*. Our unique finding is a close relationship between the physiology of tubeworm larvae and the physics of the oscillatory current regimes at the 9° 50′ N EPR site. There, the balance between larval lifespan and flow reversals can account for both larval dispersal to colonize new vent sites, and larval retention to rapidly populate an existing vent site. At our site in this region it does not appear that the dispersal distance of *R. pachyptila* is limited by the physiological performance of its larvae, but by temporal oscillations in the along-axis currents and by larval loss in cross-axis flows. Now that we have provided an estimate of the metabolic lifespan for larvae of *R. pachyptila*, dispersal distances can be predicted under the current regimes at other hydrothermal vent sites where this species occurs. □

Methods

Culture methods and measurements

Adult *Riftia pachyptila* were collected from vent sites along the EPR (9° 50′ N) and returned to the surface. In 2–3 h of arrival aboard ship, ripe eggs and sperm were removed from the gonoducts of adults at ambient pressure (1 atm), and combined for fertilization at 2 °C. The highest fertilization success rates (> 90%) were obtained by keeping

concentrated eggs and sperm together (~1,000 ml^{-1}) for 2–3 h, before transferring them to the pressure chambers at 50–100 ml^{-1}. We used standard high-performance liquid chromatography pumps and inert fittings to establish flow-through cultures in which filtered seawater was continuously replaced in a pressure vessel[23]. At the flow rates used, 90% of the column volume was exchanged in a 36-h period (that is, 1 ml min^{-1} for a 500-ml vessel with internal mixing, as verified by direct calibration). Embryos and larvae could be reared for up to 34 d using this culture system. We measured respiration rates of developing embryos using end-point assays. Embryos were transferred and maintained at pressure (250 atm) in 1-ml pressure vessels during 4–6 h incubation periods. The vessels were then depressurized and the oxygen concentration (pO_2) in the water measured at 1 atm using a microcathode oxygen sensor[9,10]. Under our conditions there was no degassing when the sample chambers were depressurized because the initial seawater oxygen concentration (O_2 solubility at 1 atm) does not increase when pressurized in our sealed system. Respiration rates were determined by transferring under pressure different numbers of embryos into the 1-ml pressure vessels, and then regressing the resultant total oxygen use against total number of individuals (Fig. 2b). The linear response over a broad range of embryo concentrations verifies that respiration rates were not impacted by concentration-dependent interactions. This method of analysis also controls for background respiration rates in the 1-ml chambers by using only the regression slope[10]. In addition, we have made respiration measurements using the low oxygen concentrations of deep-bottom water at vent sites (170 μM O_2 measured in samples collected by *Alvin* in Niskin bottles) and have found no effects on larval metabolic rates. We measured the protein content of eggs by Bradford assay with bovine serum albumin as the standard. Lipid class analyses were performed using thin layer chromatography and quantification by flame-ionization detection (Iatroscan)[24].

Buoyancy of eggs and zygotes was measured in pressurized 80-ml volume stainless steel vessels with an inside diameter of 3.2 cm. Plexiglas ports on both the top and bottom sides permitted illumination and visualization of the central 1-cm diameter portion of the water column using a dissecting microscope. All observations were done under pressure at 2 °C. After all eggs had floated to one end of the chamber, we reversed the chamber rapidly and took samples every 5 min over the following hour. At each sampling interval, the number of eggs arriving at the upper viewport was counted. Edge effects were avoided by counting only those eggs visible in the middle third of the column.

Dispersal model

The current velocities (corrected for magnetic variation) recorded at our study site varied strongly on fortnightly periods and this data record was sufficiently long to realize eight full cycles of along-axis current reversals (December 1999 to April 2000). The neutrally buoyant plume at this site was centred roughly 175-m off bottom (as reported previously[15] and as verified by our own measurements of conductivity, temperature and density (CTD/transmissometer casts). Positioning the current meters at this depth provided measurements of current regimes that were the most relevant to larval dispersal. The ridge trends NNW/SSE, at a 10° angle from geographic North, requiring the currents used for the dispersal calculations to be translated into along- and across-axis alignments. In the dispersal model, the along-axis distance x_i (in m) travelled by an individual larva released at time step i was calculated as

$$x_i = \mathrm{d}t \sum_{j=i}^{i+l-1} u_j \quad \text{for } i = 1 \text{ to } (n-l+1)$$

where dt is a 1-h time step, u_j is the mean along-axis velocity (m h^{-1}) during jth 1-h time step, n is the number of 1-h intervals in the current record, and l is the larval lifespan (h). The cross-axis distance y_i was calculated similarly, substituting the cross-axis velocity v_j for u_j. We set a limit of 25 km as the maximum distance that a larva could travel off axis and still be able to colonize the ridge. This distance corresponds roughly to the outer limit of the ridge base, and was selected because the ridge-affected flows tend to extend roughly to this distance[19,25,26]. Any larva that strayed more than 25 km off axis was excluded from further analysis.

Received 21 November 2000; accepted 1 February 2001.

1. Fornari, D. J. *et al.* Time-series temperature measurements at high-temperature hydrothermal vents, East Pacific Rise 9° 49–51′ N: monitoring a crustal cracking event. *Earth Planet. Sci. Lett.* **160,** 419–431 (1998).
2. Fornari, D. J. & Embley, R. W. in *Physical, Chemical, Biological and Geological Interactions within Seafloor Hydrothermal Systems* (eds Humphris, S. E., Zierenberg, R. A., Mullineaux, L. S. & Thomson, R. E.) 1–46 (American Geophysical Union Monograph, Washington DC, 1995).
3. Haymon, R. M. *et al.* Volcanic eruption of the mid-ocean ridge along the East Pacific Rise crest at 9° 45–52′ N: direct submersible observations of sea-floor phenomena associated with an eruption event in April, 1991. *Earth Planet. Sci. Lett.* **119,** 85–101 (1993).
4. Mullineaux, L. S., Fisher, C. R., Peterson, C. H. & Schaeffer, S. W. Tubeworm succession at hydrothermal vents: use of biogenic cues to reduce habitat selection error? *Oecologia* **123,** 275–284 (2000).
5. Lutz, R. A. *et al.* Rapid growth at deep-sea vents. *Nature* **371,** 663–664 (1994).
6. Tyler, P. A. & Young, C. M. Reproduction and dispersal at vents and cold seeps. *J. Mar. Biol.* **79,** 193–208 (1999).
7. Young, C. M., Vazquez, E., Metaxas, A. & Tyler, P. A. Embryology of vestimentiferan tube worms from deep-sea methane/sulphide seeps. *Nature* **381,** 514–516 (1996).
8. Shilling, F. M. & Manahan, D. T. Energy metabolism and amino acid transport during early development of Antarctic and temperate echinoderms. *Biol. Bull.* **187,** 398–407 (1994).
9. Marsh, A. G., Leong, P. K. K. & Manahan, D. T. Energy metabolism during embryonic development and larval growth of an Antarctic sea urchin. *J. Exp. Biol.* **202,** 2041–2050 (1999).
10. Marsh, A. G. & Manahan, D. T. A method for accurate measurements of the respiration rates of marine invertebrate embryos and larvae. *Mar. Ecol. Prog. Ser.* **184,** 1–10 (1999).
11. Evanson, M., Bornhold, E. A., Goldblatt, R. H., Harrison, P. J. & Lewis, A. G. Temporal variation in body composition and lipid storage of the overwintering, subarctic copepod *Neocalanus plumchrus* in the Strait of Georgia, British Columbia (Canada). *Mar. Ecol. Prog. Ser.* **192,** 239–247 (2000).
12. Hagen, W. & Kattner, G. Lipid metabolism of the Antarctic euphausiid *Thysanoessa macrura* and its ecological implications. *Limnol. Oceanogr.* **43,** 1894–1901 (1998).
13. Kattner, G. & Hagen, W. Lipid metabolism of the Antarctic euphausiid *Euphausia crystallorophias* and its ecological implications. *Mar. Ecol. Prog. Ser.* **170,** 203–213 (1998).
14. Cary, S. C., Felbeck, H. & Holland, N. D. Observations on the reproductive biology of the hydrothermal vent tube worm *Riftia pachyptila*. *Mar. Ecol. Prog. Ser.* **52,** 89–94 (1989).
15. Baker, E. T. *et al.* Hydrothermal plumes along the East Pacific Rise, 8° 40′ to 11° 50′ N: 1. Plume distribution and relationship to the apparent magmatic budget. *Earth Planet. Sci. Lett.* **128,** 1–17 (1994).
16. Lupton, J. E. *et al.* Tracking the evolution of a hydrothermal event plume with a RAFOS neutrally buoyant drifter. *Science* **280,** 1052–1055 (1998).
17. Kim, S. L., Mullineaux, L. S. & Helfrich, K. Larval dispersal via entrainment into hydrothermal vent plumes. *J. Geophys. Res.* **99,** 12655–12665 (1994).
18. Mullineaux, L. S., Wiebe, P. H. & Baker, E. T. Larvae of benthic invertebrates in hydrothermal vent plumes over Juan de Fuca Ridge. *Mar. Biol.* **122,** 585–596 (1995).
19. Thomson, R. E., Roth, S. E. & Dymond, J. Near-inertial motions over a mid-ocean ridge: effects of topography and hydrothermal plumes. *J. Geophys. Res.* **95,** 12961–12966 (1990).
20. Cannon, G. A. & Pashinski, D. J. Variations in mean currents affecting hydrothermal plumes on the Juan de Fuca Ridge. *J. Geophys. Res.* **102,** 24965–24976 (1997).
21. Crane, K., Aikman III, F. & Foucher, J.-P. The distribution of geothermal fields along the East Pacific Rise from 13° 10′ N to 8° 20′ N: implications for deep seated origins. *Mar. Geophys. Res.* **9,** 211–236 (1988).
22. Chevaldonné, P., Jollivet, D., Vangriesheim, A. & Desbruyères, D. Hydrothermal-vent alvinellid polychaete dispersal in the eastern Pacific . 1. Influence of vent site distribution, bottom currents, and biological patterns. *Limnol. Oceanogr.* **42,** 67–80 (1997).
23. Jannasch, H. W., Wirsen, C. O. & Doherty, K. W. A pressurized chemostat for the study of marine barophilic and oligotrophic bacteria. *Appl. Environ. Microbiol.* **62,** 1593–1596 (1996).
24. Miller, C. B., Morgan, C. A., Prahl, F. G. & Sparrow, M. A. Storage lipids of the copepod *Calanus finmarchicus* from Georges Bank and the Gulf of Maine. *Limnol. Oceanogr.* **43,** 488–497 (1998).
25. Thomson, R. E., Gordon, R. L. & Dymond, J. Acoustic doppler current profiler observations of a mid-ocean ridge hydrothermal plume. *J. Geophys. Res.* **94,** 4709–4720 (1989).
26. Cannon, G. A., Pashinski, D. J. & Lemon, M. R. Mid-depth flow near hydrothermal venting sites on the southern Juan de Fuca ridge. *J. Geophys. Res.* **96,** 12815–12831 (1991).

Acknowledgements

We thank the captain and crew of the RV *Atlantis II*, and the support crew of the DSV *Alvin*. We acknowledge the data collection and assistance of S. Brooke, A. Green, S. Mills, M. Moore and D. Pace. C. Allen, S. Beaulieu, T. Griffin, H. Hunt, A. Metaxas, P. Tyler and J. Welch provided assistance at sea; M. Grosenbaugh provided programming and conceptual assistance with the dispersal model. This work was supported by grants from the National Science Foundation.

Correspondence and requests for materials should be addressed to D.T.M. (e-mail: manahan@usc.edu).

Foci of orientation plasticity in visual cortex

Valentin Dragoi*, Casto Rivadulla*† & Mriganka Sur*

* *Department of Brain and Cognitive Sciences and Center for Learning and Memory, Massachusetts Institute of Technology, Cambridge, Massachusetts 02139, USA*

Cortical areas are generally assumed to be uniform in their capacity for adaptive changes or plasticity[1–4]. Here we demonstrate, however, that neurons in the cat striate cortex (V1) show pronounced adaptation-induced short-term plasticity of orientation tuning primarily at specific foci. V1 neurons are clustered according to their orientation preference in iso-orientation domains[5] that converge at singularities or pinwheel centres[6,7]. Although neurons in pinwheel centres have similar orientation tuning and responses to those in iso-orientation domains, we find that they differ markedly in their capacity for adaptive changes.

† Present address: Neuroscience and Motor Control Group (NEUROcom), E U Fisioterapia, Campus de Oza, 15006 A Coruna, Spain.